Article:

Barattucci, S, Sarhosis, V orcid.org/0000-0002-8604-8659, Bruno, AW et al. (3 more authors) (2020) An experimental and numerical study on masonry triplets subjected to monotonic and cyclic shear loadings. Construction and Building Materials, 254. 119313. ISSN 0950-0618

https://doi.org/10.1016/j.conbuildmat.2020.119313

AN EXPERIMENTAL AND NUMERICAL STUDY ON MASONRY TRIPLETS SUBJECTED TO MONOTONIC AND CYCLIC SHEAR LOADINGS

Samuel Barattucci[1,3], Vasilis Sarhosis[2*], Agostino Walter Bruno[3], Antonio Maria D'Altri[1], Stefano de Miranda[1], Giovanni Castellazzi[1]

[1] Department of Civil, Chemical, Environmental, and Materials Engineering (DICAM), University of Bologna, Bologna, Italy

[2] School of Civil Engineering, University of Leeds, Leeds, United Kingdom

[3] School of Civil Engineering, University of Newcastle, Newcastle Upon Tyne, United Kingdom

ABSTRACT

This paper presents an experimental and numerical study on the mechanical behaviour of masonry triplets subjected to monotonic and cyclic shear loadings. Masonry triplets were constructed with fired bricks bonded together with three different in composition (i.e. cement-to-sand ratios) mortars. Shear tests on triplets show that cyclic loading significantly reduces the peak shear strength (typically around 18%) with respect to monotonic loads, regardless of the mortar composition. The shearing behaviour of the triplets obtained from the experiments were successfully reproduced using an innovative discrete element modelling strategy in which masonry units and mortar were represented by a series of irregular particles (i.e. through Voronoi-shaped particles) with a fictitious random microstructure. Numerical results highlight that cyclic shear strength reduction can be attributed to the progressive formation of cracks in the mortar layers along with the cyclic loading. These observations provide new insight into behaviour of structural masonry and lead to suggestions for improving assessment techniques for masonry structures subjected to combined actions of compression and shear.

*Corresponding author: Dr Vasilis Sarhosis, School of Civil Engineering, University of Leeds, Leeds, United Kingdom, email: v.sarhosis@leeds.ac.uk

***KEYWORD*S**: *Masonry; triplets; monotonic shear; cyclic shear; discrete element method; material parameters.*

HIGHLIGHTS

- Monotonic and cyclic shear loadings were applied on masonry triplets
- Mortar composition and compression levels affect shearing behaviour of triplets
- Peak shear strength reduces during cyclic loadings
- DEM simulations well reproduce experimental results
- Shear strength reduction is driven by the progressive formation of micro-cracks in mortar

1. *INTRODUCTION*

Masonry is a construction material that is very common worldwide. Masonry structures have been used for millennia due to its ease of construction, simplicity, low costs, and durability. Masonry can be generally defined as a composite material, made of natural or artificial elements assembled in various patterns and bonded together with or without mortar (Bui et al., 2017). From the mechanical point of view, masonry is a heterogeneous, nonlinear and anisotropic material, consisting of masonry units, mortar and masonry unit-to-mortar interfaces. Also, masonry is characterized by its very low tensile strength, substantial strength in compression and weak performance in bending and shear. Indeed, it is well known that masonry buildings are weak against horizontal actions (e.g. earthquakes). Tensile and shear bond strengths are quite low and highly variable. Thus, masonry walls fail mostly through masonry unit-to-mortar interfaces, known as planes of weakness (Ferretti et al., 2019).

Several numerical and experimental studies have been carried out in the past to understand the non-linear behaviour of masonry subjected to in-plane and out of plane loading (Bertolesi et al. 2018; Bertolesi et al. 2016; Silva et al. 2017; Bertolesi et al. 2019). The material properties which affect the response of shear walls are typically the properties of masonry units, the masonry unit-to-mortar bond and friction (Sarangapani et al., 2005; Sarhosis and Sheng, 2014). Since the strength of a masonry wall depends on the bond between masonry units and mortar and on the mortar properties (Dehghan et al., 2018), an understanding of the behaviour of this composite material requires the characterization of its components (Livitsanos et al., 2019). Indeed, the properties of masonry are strongly dependent upon the properties of its constituents (Franzoni et al., 2014). Masonry units/blocks and mortar are quasi-brittle materials, which typically fail due to a process of progressive internal crack growth (Lourenço et al., 2004). An adequate characterization of both the single components and the bond between mortar and masonry units is needed for an effective structural analysis of masonry structures and should be performed through extensive experimental testing (Milosevic et al., 2013).

The allowable pre-compression level is another important factor that influences the masonry elements in-plane shear strength and deformability (Abdou et al., 2006). Indeed, normal compressive stresses acting on the interface affect both the peak shear stress and residual strength in a rather similar way (Rahman and Ueda, 2013), given that this process is typically governed by a frictional behaviour. Capozucca (2011) reported that the shear strength of a masonry wall increases with the pre-compression up to a limit and become constant at higher compression levels. Furthermore, increasing the compression level may lead to a decrease in the shear strength and ultimate drift due to the failure in compression (Capozucca, 2017). Zhuge (1998) developed discrete element models of masonry construction and has reported that the tensile and shear bond strengths of masonry have more influence when the pre-compression level is low.

Triplet shear test allows to determine the in-plane shear strength of horizontal bed joints in masonry, according to standards BS EN 1052-3:2002. Except for the study carried out by Mojsilović et al. (2015), only monotonic application of the shear action on triplets has been conducted so far (Pelà et al., 2017). Particularly, monotonic and static-cyclic shear tests on masonry with multi-layer bed joints were presented in Mojsilović et al. (2015), where extruded elastomer membranes (Mojsilović et al., 2019) were employed in the joints to prevent and limit the deterioration of the core soft layer during the cycling action (Mojsilović, 2012). Other cyclic tests (Lin et al., 2017) were limited to dry stack masonry joints, where only friction (without cohesion) exists.

This paper aims to provide an understanding on how the different monotonic and cyclic loading can affect the shear strength of a masonry triplet. Such investigation is anticipated to give a better understanding of the performance of masonry structures subjected to repeated loading conditions in shear. Both monotonic and cyclic shear test on the masonry triplets were undertaken. Masonry triplets were constructed with three different mortar compounds and tested at three different level of pre-compression load, so allowing to study the influence of the mortar properties on ultimate strength (Alecci et al., 2013).

It is well known that numerical models can be very useful to mechanically interpret experimental outcomes. This is especially true when dealing with masonry structures/assemblages (D'Altri et al., 2019) given the broad variability of the material response (Andreotti et al., 2018) and its significant complexity (Casolo and Milani, 2013). So, in this study, experiments carried out in the laboratory were numerically simulated by means of a non-standard discrete element modelling (DEM) strategy based on a fictitious random microstructure of units and mortar (Sarhosis and Lemos, 2018). This advanced numerical model reproduces the heterogeneity and discontinuity of mortar as an assemblage of voronoi-shaped particles. In this way, initiation and propagation of cracking in the mortar, brick and brick-to-mortar interface can be obtained. Experimental and numerical results are compared and critically discussed.

The paper is organized as follows. Section 2 describes the experimental campaign carried out in this study. Section 3 describes the numerical modelling strategy adopted and its implementation to simulate the experimental tests. Section 4 collects the results discussion, i.e. the experimental and numerical results are compared and critically discussed. Finally, Section 5 outlines the conclusions of this study.

2. EXPERIMENTAL CAMPAIGN

2.1 Mortars and individual bricks characterization

Masonry triplets were manufactured by bonding standard fired bricks with different cement-based mortars mixed at the three cement to sand ratios of 1:3, 1:6 and 1:9 (named hereafter as mortars 1:3 MC, 1:6 MC and 1:9 MC). The mortar 1:9 MC reproduces old masonry constructions with weak bonding properties (Sarhosis and Sheng, 2014) while the other two compositions simulate modern masonry constructions (Rahman & Ueda 2013). The mortars 1:3 MC, 1:6 MC and 1:9 MC were respectively mixed with the three water to cement ratios of 0.9:1, 1.3:1 and 1.5:1 to ensure cement hydration and lubrication of sand particles. These water/cement ratios correspond to the lowest amount of water required to attain suitable workability and a good mechanical performance. This was confirmed by slump tests, which showed that the mortars 1:3 MC, 1:6 MC and 1:9 MC achieved medium workability with slump equal to 53, 58 and 61 mm. Similar to Singh et al. (2015), a larger amount of water was necessary for mortars with higher sand content. A total of 33 masonry triplets were manufactured with 11 samples for each mortar composition.

To characterise the mechanical behaviour of the different mortars, a total of 9 mortar specimens (i.e. 3 specimens for each cement to sand ratio) were casted in normalized mould of 40 x 40 x 160 mm^3, as shown in Figure 1a. Mortar specimens were then left 28 days at a temperature of about 25 °C for curing and subsequently subjected to three-point bending tests performed at a constant displacement rate of 0.05 mm/min. The flexural strength f_{vk} of all mortar samples was calculated from the three-point bending test as prescribed by the EN 1015-11 (1999) as follows:

$$f_{vk} = \frac{3}{2} \frac{R_f \, l}{bh^2} \tag{1}$$

where R_f is the peak load, l is the span between the supports, b and h are the width and height of the vertical cross-section of the mortar sample, respectively. After the three-point bending test, one of the two halves of the failed samples (Figure 1b) was collected and then subjected to compressive strength tests at a constant displacement rate of 0.10 mm/min. The Young's modulus E of each mortar sample was calculated from compressive strength tests by assuming a linear elastic response for compressive stresses between 5% and 33% of the peak strength f_c (Drysdale et al., 1999; ASTM C1314-03b, 2003). The Shear modulus G was instead calculated as the 40% of the Young's Modulus, as indicated by Lekhnitskii (1963) and various national masonry building codes including the Eurocode 6 (2005).

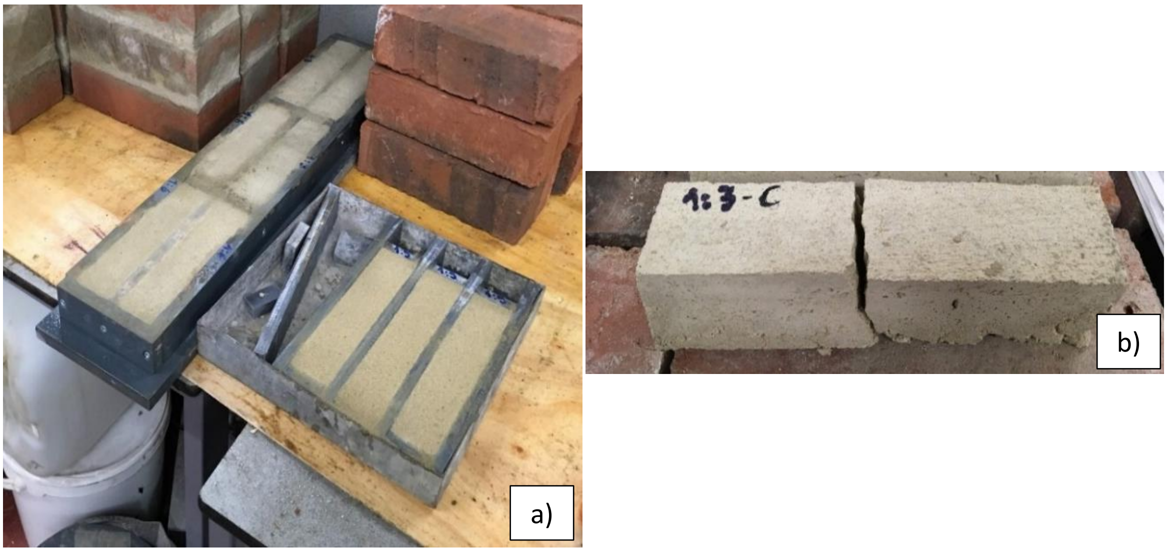

Figure 1. Mortar specimens used for the three-point bending test (a) and failed samples after three-point bending test (b).

Figures 2 and 3 show the three-point bending and compressive tests results, respectively. The notations *a*, *b* and *c* indicate the three different specimens tested for each mortar composition. The strain values shown in Figure 3 were calculated as per variation of sample height, which was measured by the vertical displacement of the press plate, divided by the initial height of the sample. Figures 2 and 3 show that both stiffness and strength increase with increasing cement to sand ratio. Also, compressive peak strengths occurred at increasingly higher strains, as the cement to sand ratio increased (Figure 3). After the peak strength was reached, all samples exhibited a brittle failure which is more evident during the three-point bending tests (Figure 2), rather than compressive tests (Figure 3). Table 1 summarises the average values of material properties for each mortar composition together with the corresponding values of standard deviation (in brackets).

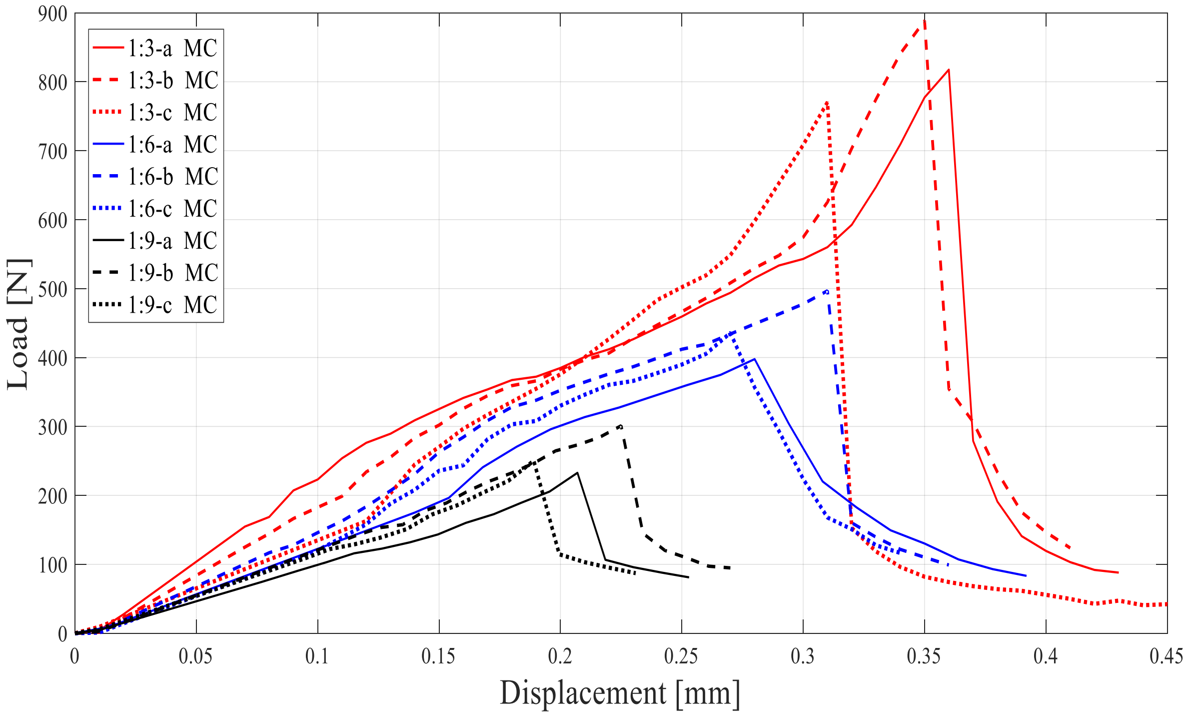

Figure 2. Results from three-point bending tests on mortar samples with different cement to sand ratios.

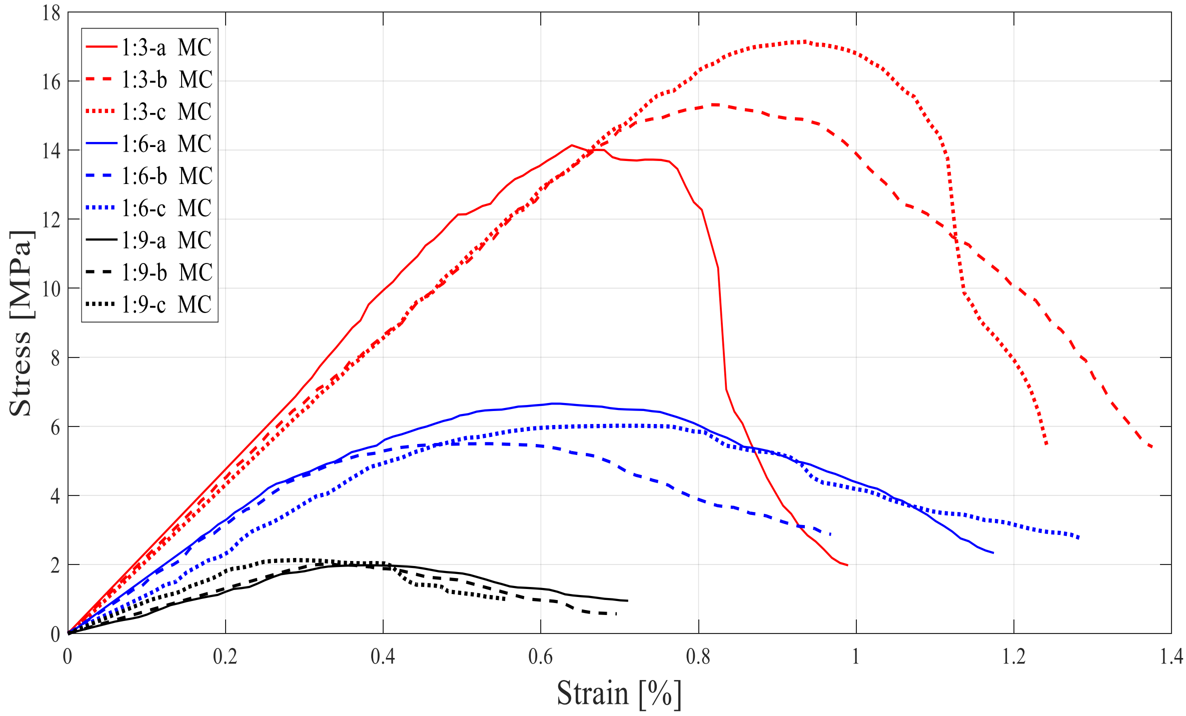

Figure 3. Results from compressive strength tests on mortar samples with different cement to sand ratios.

Table 1. Mechanical tests on mortar samples and corresponding standard deviation (in brackets)

		Three-point bending test		Compressive strength test		
Mortar	**Density [kg/m^3]**	**R_f [N]**	**f_f [MPa]**	**f_c [MPa]**	**E [GPa]**	**G [GPa]**
1:3	1943 (18)	826 (48)	2.77 (0.23)	15.57 (1.2)	2.19 (0.13)	0.88 (0.05)
1:6	1794 (9)	443 (41)	1.44 (0.10)	6.06 (0.48)	1.46 (0.13)	0.58 (0.05)
1:9	1698 (22)	256 (35)	0.80 (0.09)	2.04 (0.06)	0.72 (0.12)	0.29 (0.05)

The three mortars 1:3 MC, 1:6 MC and 1:9 MC were used to bond together standard fired bricks named by the supplier JT Dove as “Birtley Old English Bricks”. Bricks had dimensions of 215 x 102.5 x 65 mm^3, as shown in Figure 4a. The strength properties of the bricks were not investigated in the present experimental campaign, given that masonry triplets substantially showed failure in the mortar joints, i.e. there was no failure of the bricks. Note that the largest faces of the bricks, which are in contact with the mortar joints in the masonry triplets, exhibited different roughness with one side being much rougher than the other (Figures 4b and 4c). Hence, prior to triplets manufacturing, the smooth largest face of the brick was scarified to obtain similar conditions on both sides of the mortar joints. However, to limit this artificial adjustment, the rough side of the two external bricks was always oriented towards the mortar joints so that only one side of the intermediate brick was scarified.

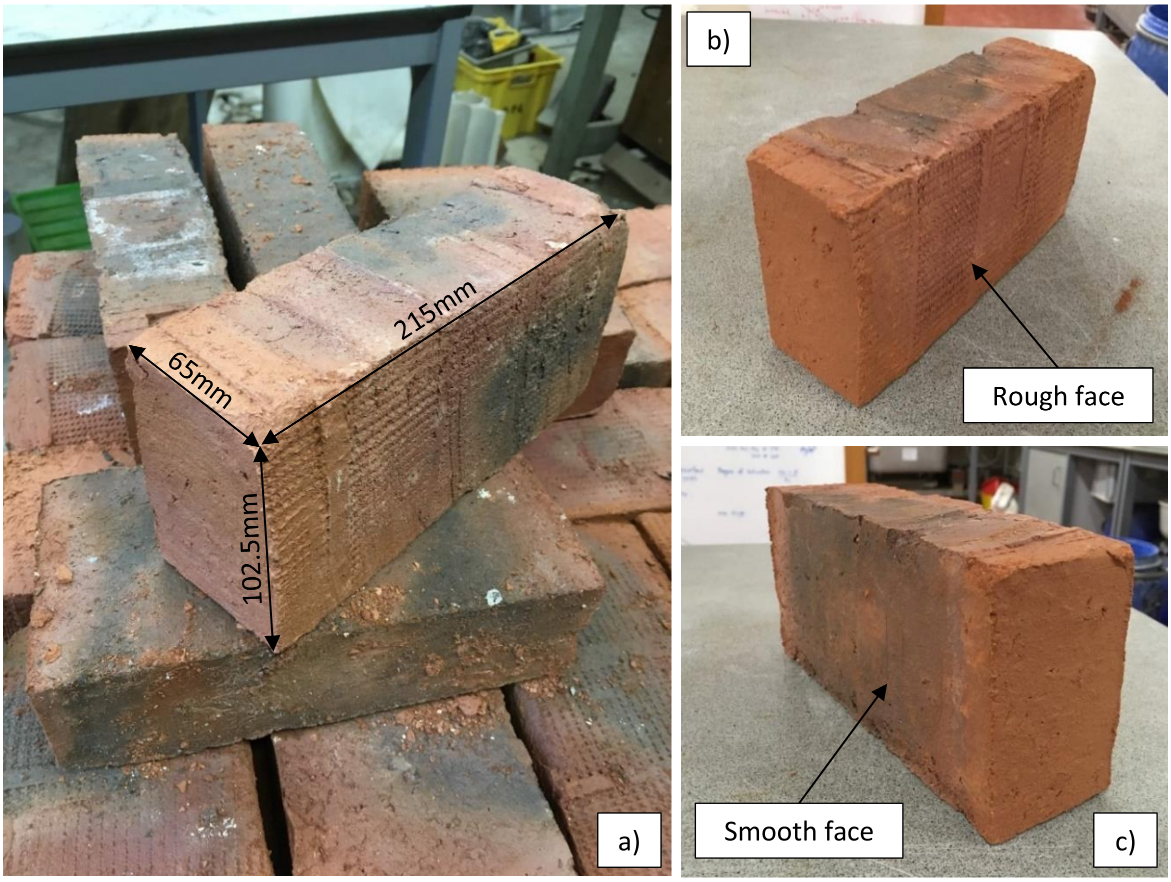

Figure 4. Typical Birtley old English bricks used in this experimental study: brick dimensions (a), rough (b) and smooth (c) faces of the bricks.

2.2 Manufacturing of masonry triplets and experimental tests set-up

Each masonry triplet was manufactured with three bricks bonded together by two 10 mm-thick mortar joints, as shown in Figure 5, leading to masonry triplets with dimensions of 215 x 215 x 102.5 mm^3 (Figure 5a). Prior to manufacturing, all bricks were submerged in water for a minimum time of 24 hours to ensure an optimised bonding with the mortar joints and to avoid quick drying of the samples with a consequent formation of cracks. Bricks were then wiped with a dry cloth before proceeding with the laying of the mortar joints. Special care was taken to build the masonry triplets as straight as possible to avoid spurious eccentricities that could affect the shearing tests. After manufacturing, masonry triplets were left to cure for a minimum time of 28 days in laboratory at a temperature of about 25°C (Figure 5b).

Figure 5. Typical masonry triplet showing dimensions (a) and curing of all samples in laboratory (b).

After curing, masonry triplets were subjected to shear mechanical tests to investigate the effect of mortar compositions and compression levels on the shearing behaviour of masonry elements. The basic shear test set-up proposed by the European Standard EN 1052-3 (2002) was modified during the present experimental campaign to perform both monotonic and cyclic shearing tests on masonry triplets, as shown in Figure 6. Therefore, the novelty of the proposed testing apparatus consists in the possibility of applying shear loadings in both downward and upward directions (Figure 6).

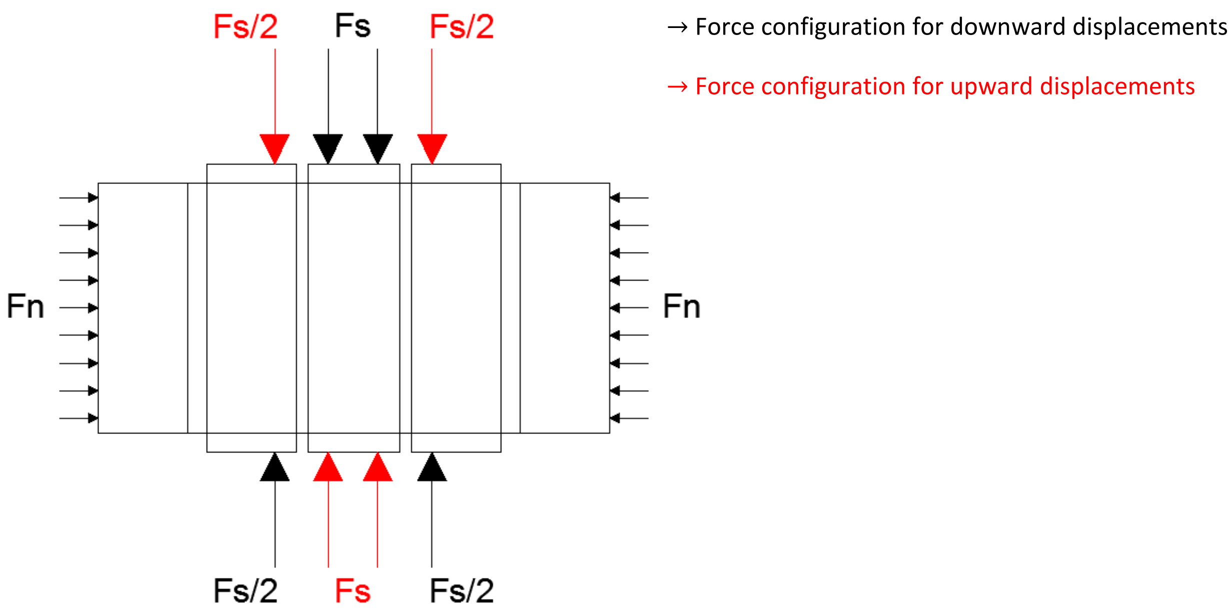

Figure 6. Shear test set-up: forces configuration.

The assembly of the testing apparatus is here described by considering the numbering of the parts shown in Figure 7:

- Two pairs of threaded rods (2) and a sequence of two thick plates (3a), two cylindrical rods (4) and two thin plates (5) are firstly fixed to the aluminium base (1). This sequence of plates and pistons serves to punctually transfer the load on the two external bricks.
- A system of two threaded rods (6) with a thick plate (3b), two cylindrical rods (4) and a thin plate (5) is then placed on a temporary support between the two pairs of threaded rods (2) without being fixed to the aluminium base. This system will apply the shear loading to the intermediate brick during testing.
- The masonry triplet is then positioned on the thin plates (5) and a specular system of plates and cylindrical pistons is mounted on top of the triplets.
- The system of threaded rods, plates and cylindrical pistons fixed to the intermediate brick is finally connected to the press by means of a centring device (7) so that the temporary support placed below could be removed.

An independent system was used to apply the horizontal compressive stress on masonry triplets. This system consisted in a frame made of two steel tubular profiles (10) placed at the two sides of the triplet and assembled by two threaded rods (11). This frame held in place a pressure jack (12), a sequence of two IPE profiles (8) and two plywood boards (9) (Figure 7). The compressive stress was applied before the shearing loading and kept constant during the entire duration of the test. Figure 8 shows the assembled equipment used to perform the shear tests on masonry triplets.

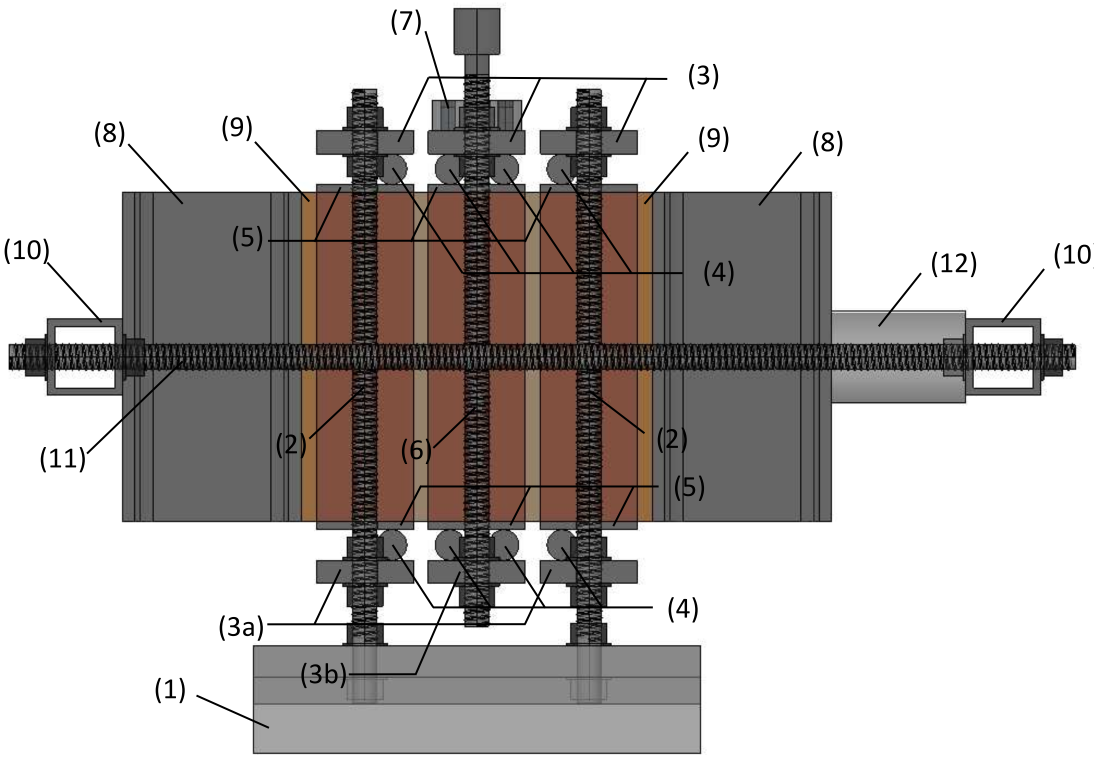

(1) aluminium base	*(7) centering device*
(2) threaded rods	*(8) IPE profiles*
(3) thick steel plates	*(9) plywood boards*
(4) cylindrical rods	*(10) steel tubular profiles*
(5) thin plates	*(11) threaded rods*
(6) threaded rods	*(12) pressure jack*

Figure 7. Testing equipment apparatus used to perform shearing tests on triplet specimens.

Figure 8. Assembled equipment for shear testing.

The testing programme consisted of performing monotonic shearing on three triplets for each of the three mortar compositions (1:3, 1:6 and 1:9 MC), one for each of the three levels of confinement (0.2, 0.6 and 1 MPa), for a total of nine masonry triplets tested in monotonic conditions. Then, similarly for the monotonic shear tests, cyclic shearing was performed on other nine masonry triplets.

2.2.1 Monotonic shear tests

Monotonic shear tests were performed by means of the computer-controlled press INSTRON with a maximum load capacity of 250 kN. The shear loading was applied with a constant displacement rate of 1 mm/min. Table 2 summarises both peak and residual shear loads (indicated as P_{RM} and r_{RM}, respectively) the masonry triplets exhibited during monotonic shearing, for different levels of precompression, σ_{hp}, and different mortar compositions.

Table 2. Peak and residual loads of masonry triplets subjected to monotonic shear tests

Mortar	σ_{hp} [MPa]	P_{RM} [kN]	r_{RM} [kN]
1:3	1	87.49	54.21
	0.6	67.21	32.24
	0.2	50.90	11.75
1:6	1	80.61	48.68
	0.6	60.44	27.55
	0.2	44.78	11.81
1:9	1	56.11	40.83
	0.6	41.58	23.99
	0.2	23.28	11.83

Figure 9 shows the relationship between the shear strengths, calculated as the ratio between the peak and residual shear strength and the area of the two vertical cross-sections passing through the mortar joints, and the precompression stress for all masonry triplets built with the three mortars 1:3 MC, 1:6 MC and 1:9 MC. Experimental data can be easily interpolated with straight lines that represent the Mohr-Coulomb criterion expressed as:

$$\tau = c + \sigma_{hp} tan(\phi) \tag{2}$$

where τ is the shear strength, c is the cohesion, and ϕ is the friction angle. Table 3 shows the values of both cohesion and friction angle calculated from the trendlines shown in Figure 9 for peak and residual shear strength. Note that the residual cohesion is set to zero to represent that, after the cracking of both mortar joints, the shear resistance is purely due to friction. As can be noted from Table 3, the values of residual friction angle are slightly higher than the peak ones. This suggests a stronger effect of the precompression stress on the post-peak resistance compared with the peak strength. Also, the Morh-Coulomb interpolation is only acceptable in the low range of precompression stress, as it will erroneously predict a residual shear strength higher than the peak one for sufficiently high levels of precompression stress. Conversely, it can be hypothesised that the residual shear strength would eventually tend towards the peak strength at the high range of precompression stress.

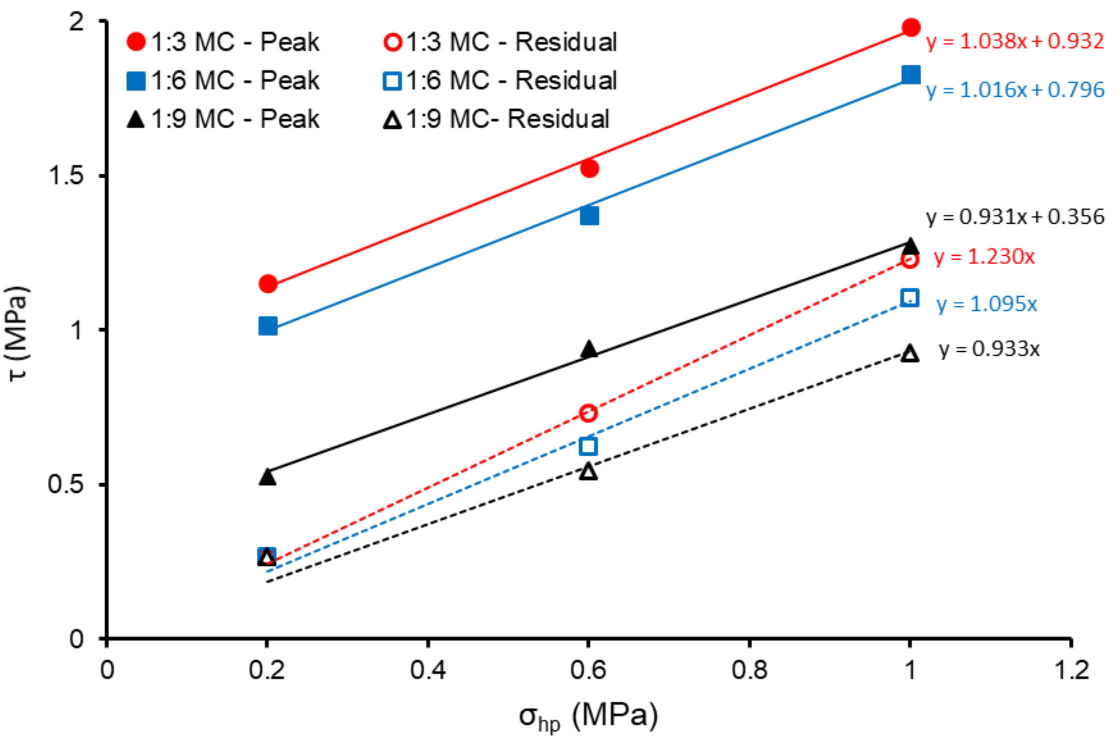

Figure 9. Relationship between shear strength and precompression stress for masonry triplets built with mortars 1:3 MC, 1:6 MC and 1:9 MC.

Table 3. Peak and residual values of cohesion and friction angle for all masonry triplets

Mortar	c [MPa]	ϕ [°]	c_{res} [MPa]	ϕ_{res} [°]
1:3	0.932	46.1	0	50.9
1:6	0.796	45.5	0	47.6
1:9	0.356	43.0	0	43.0

2.2.2 Cyclic shear tests

Masonry triplets were also subjected to cyclic shear tests at the three horizontal precompression stresses of 0.2, 0.6 and 1 MPa and with a vertical shear load applied at a constant displacement rate of 1 mm/min. Figure 10 shows the experimental protocol followed to perform cyclic shear tests. Shear loading was applied by alternatively imposing downward and upward displacements on the intermediate brick over ten cycles. The imposed displacement was increased at each cycle by 10% of the displacement that corresponded to the peak strength measured during monotonic tests. The last cycle was continued until the failure of the masonry triplet was reached.

Table 4 summarises results of peak shear loads (P_{RC}) measured during cyclic tests together with the peak load variation respect to the monotonic tests. As it can be noted, a significant decrease of peak shear load is observed for cyclic tests with respect to monotonic tests. Particularly, most of the specimens showed a peak shear load decrease greater up to 39%, while no peak shear load decrease is observed in only two cases (Table 4).

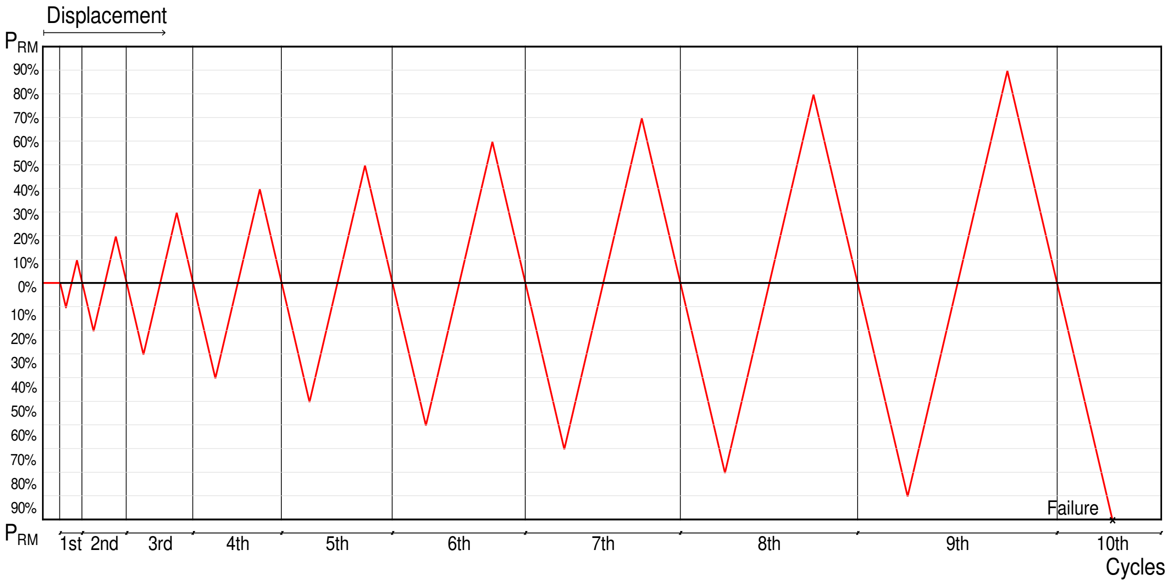

Figure 10. Experimental procedure followed for the cyclic tests.

Table 4. Peak shear load of masonry triplets subjected to cyclic tests and comparison with monotonic tests

Mortar	σ_{hp} **[MPa]**	P_{RC} **[kN]**	$P_{RC} - P_{RM}$ **[kN]**	$\frac{P_{RC}-P_{RM}}{P_{RM}}$ **[%]**	**Average variation [%]**
1:3	1.0	88.12	+0.63	+0.7%	-15.8
	0.6	48.98	-18.23	-27%	
	0.2	40.01	-10.89	-21%	
1:6	1.0	84.26	+3.65	+4.5%	-19.8
	0.6	45.46	-14.98	-25%	
	0.2	27.02	-17.76	-39%	
1:9	1.0	44.10	-12.01	-21%	-17.7
	0.6	36.90	-4.68	-11%	
	0.2	18.41	-4.87	-21%	

3. NUMERICAL MODELING

3.1 Overview of the discrete element method for modelling masonry

A discrete element modelling strategy based on a fictitious random microstructure of units and mortar, originally developed by Sarhosis and Lemos (2018), was used to get more insights on the mechanical behaviour of masonry triplets subjected to shear. Particularly, mortar bed joints were subdivided into Voronoi-shaped elements, which were then subdivided into simple triangular finite elements behaving in a linear elastic isotropic manner. Voronoi-shaped elements were bonded together by zero-thickness interfaces. Figure 11 shows the masonry units and mortar bed joints represented by voronoi-shaped elements. The numerical model has been implemented in the two-dimensional software UDEC based on the discrete element method (Itasca, 2004). For further information and applications of the discrete element method for modelling masonry, the reader is directed to Sarhosis et al. (2016).

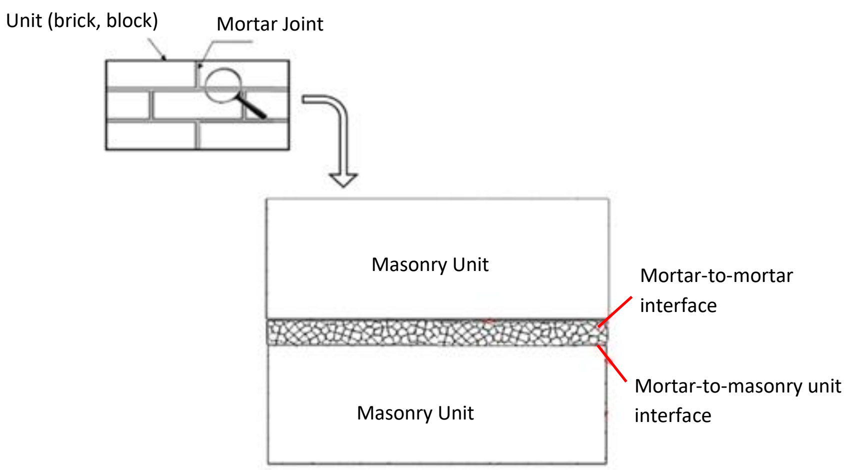

Figure 11. Representation of masonry units and mortar bed joints represented by voronoi-shaped elements.

The mechanical interaction between Voronoi elements is shown in Figure 12. Within the model and at each time-step, forces in the normal and shear direction were governed by the following equations:

$$\Delta F^n = -jK_n \, \Delta U_n \, A_c \qquad (3)$$

$$\Delta F^s = -jK_s \, \Delta U_s \, A_c \qquad (4)$$

where ΔF^n, ΔF^s are the normal and the shear force increment (resultant for the contact point); jK_n, jK_s the joint normal and the joint shear stiffness; ΔU_n, ΔU_s the normal and the shear contact displacement increments, defined as the relative displacements between the two blocks at the contact point; and A_c the area related to the contact point.

At interfaces, Mohr-Coulomb failure surface with tension cut-off is assigned. This assumes limit tensile and shear strength, with a brittle failure followed by a sudden drop from peak to residual strength as soon as either normal or shear failure takes place, see Figure 13. The model has a limiting tensile strength, $Jten$, defined by the user. If the normal stress ($\sigma_n = F^n/A_c$, positive in tension) reaches the tensile strength ($\sigma_n = Jten$), then the normal tensile stress is set to zero ($\sigma_n = 0$) and the interface opens. Figure 13 shows the joints constitutive laws used in the present study. In the shear direction, the model uses the explicit incorporation of Coulomb's frictional behaviour. Thus, slippage between bricks will occur when the shear stress ($\tau_s = F^s/A_c$) at the interface reaches a critical value τ_{max} defined by:

$$\tau_{max} = Jcoh - \sigma_n \tan(Jfric) \qquad (5)$$

where $Jfric$ is the friction angle and $Jcoh$ the cohesive strength. After reaching the critical value τ_{max}, the shear stress is set to be equal to $\tau_r = \sigma_n \tan(Jfric)$ The Mohr-Coulomb with tension cut-off criterion used in this study has been widely used by researchers to model the mechanical behaviour of masonry (e.g. D'Altri et al., 2018; Lourenço, 2002; Milani, 2011).

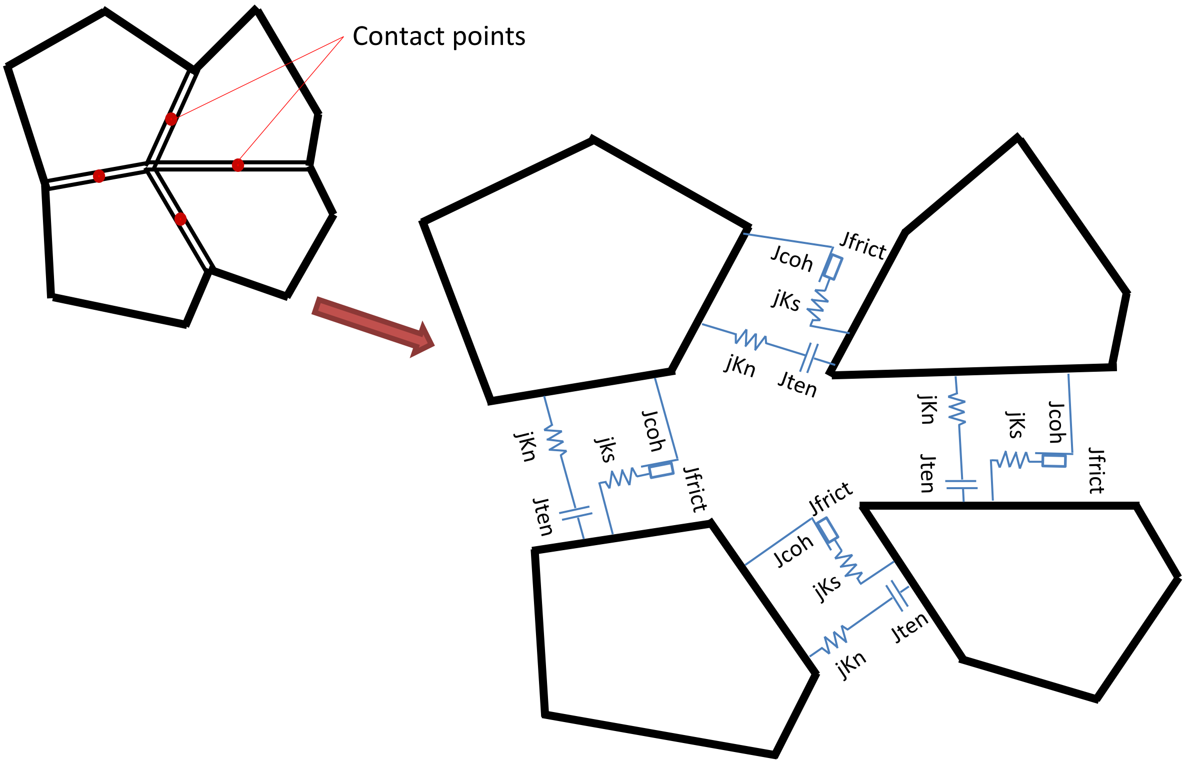

Figure 12. Mechanical representation of the interaction between voronoi elements (Sarhosis & Lemos 2018)

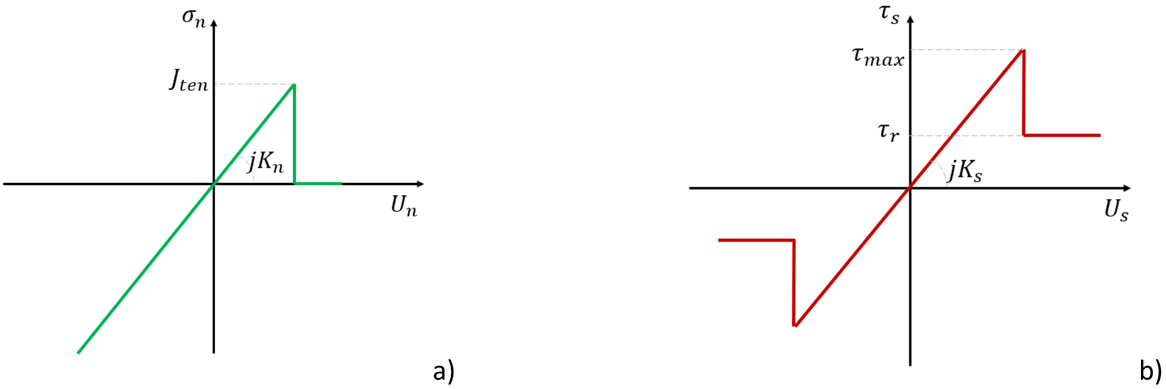

Figure 13. Joints constitutive laws used in the present study (a) joint behavior in the normal direction; and (b) joint behaviour in the shear direction (Itasca 2004)

3.2 Development of the DEM computational model for the shear tests on masonry triplets

Geometric models to represent masonry triples were created in UDEC software. The geometry of the masonry triplets is shown in Figure 14. The two-dimensional model developed herein simulates plain strain conditions. Mortar joints were represented by a series of Voronoi elements and were also modelled as a series of deformable blocks. The shape of the Voronoi elements were created randomly. However, a constant length has been assigned to all Voronoi elements. Properties of the mortar were obtained from Section 2.1 and Table 1, while bricks have been considered as rigid blocks. The calibrated material properties of the masonry unit-to-mortar and mortar-to-mortar interfaces used for the development of the computational model are shown in Tables 5 and 6. From the material parameter calibration study, it was found that the cohesive and tensile strength of the mortar-to-mortar interface is double to the one of the brick-to-mortar interface. Values of friction and angle and residual friction angle for both masonry unit-to-mortar and mortar-to-mortar interfaces were taken from the experimental study (see Table 3). Also, dilation angle, J_{dil}, was taken as 10 degrees in all cases (Van der Pluijm 1993). In fact, the size and geometry of the Voronoi elements will contribute to the global dilation at the joint. However, a full investigation on the effect of the geometry and size of Voronoi elements on the global dilation of the mortar joint is not part of this study.

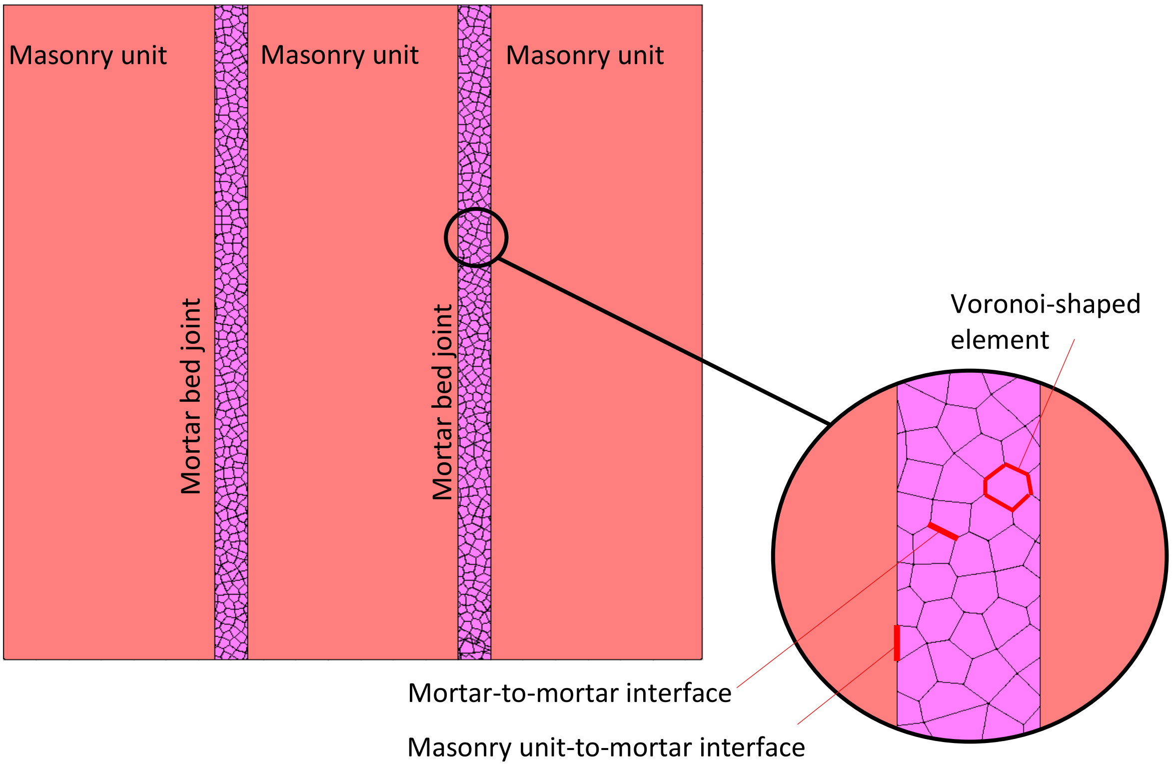

Figure 14. Representation of masonry triplets by means of voronoi elements.

Table 5 – Input parameters (both peak and residual) used on the masonry unit-to-mortar interface.

Mortar	Jk_n [GPa]	Jk_s [GPa]	$Jfrict$ [°]	$Jrfrict$ [°]	$Jcoh$ [MPa]	$Jrcoh$ [MPa]	$Jten$ [MPa]	$Jdil$ [°]
1:3	23	6.0	46.1	50.3	3.26	0.07	3.26	10
1:6	23	6.5	45.5	46.3	2.79	0.13	2.79	10
1:9	23	3.5	43.0	39.4	1.25	0.30	1.25	10

Table 6 – Input parameters (both peak and residual) used on the mortar-to-mortar interface.

Mortar	Jk_n [GPa]	Jk_s [GPa]	$Jfrict$ [°]	$Jrfrict$ [°]	$Jcoh$ [MPa]	$Jrcoh$ [MPa]	$Jten$ [MPa]	$Jdil$ [°]
1:3	23	6.0	46.1	50.3	6.52	0.14	6.52	10
1:6	23	6.5	45.5	46.3	5.58	0.26	5.58	10
1:9	23	3.5	43.0	39.4	2.50	0.60	2.50	10

3.2.1 Application of load - monotonic shear tests and cyclic shear tests

A vertical velocity was assigned at the top of the middle brick of the triplet. This was to reproduce the displacement controlled test performed in the laboratory. Converge tests carried out so that a quasi-static response is achieved in the model. The velocity imposed at the middle brick of each triplet speciment was equal to 0.001 mm/s. Cyclic shear was imposed by applying a constant velocity on the middle break in both upward and downward vertical directions. The imposed velocity was, similar in magnitude to the monotonic tests and equal to 0.001mm/s. The model test protocol was the same of the experimental test. A FISH function (internal programming language of UDEC) has been written. The FISH function was able to record the reaction forces from the fixed velocity grid-points acting on the middle brick of the triplet at each time step. Such conditions were selected to replicate the conditions of the experimental loading test carried out in the laboratory.

4. RESULTS DISCUSSION

In this section, the experimental and numerical results are compared and critically discussed for both monotonic and cyclic shear tests on masonry triplets.

4.1 Monotonic shear tests

Figures 15, 16 and 17 show the comparison between experimental and numerical results of monotonic shear tests performed on masonry triplets made with the mortars 1:3 MC, 1:6 MC and 1:9 MC, respectively. According to the testing programme, for each mortar composition, three different samples were tested at three different horizontal pre-compression stresses σ_{hp} of 0.2, 0.6 and 1 MPa.

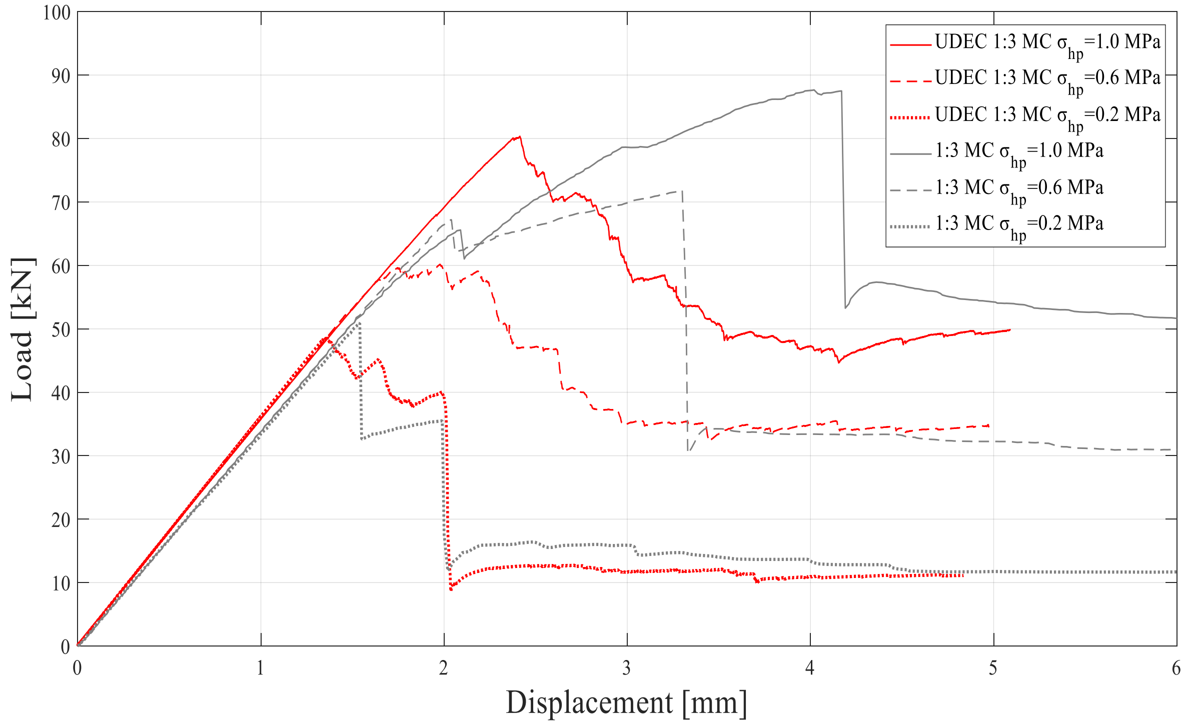

Figure 15. Experimental and numerical results of monotonic shear test on triplet with 1:3 MC

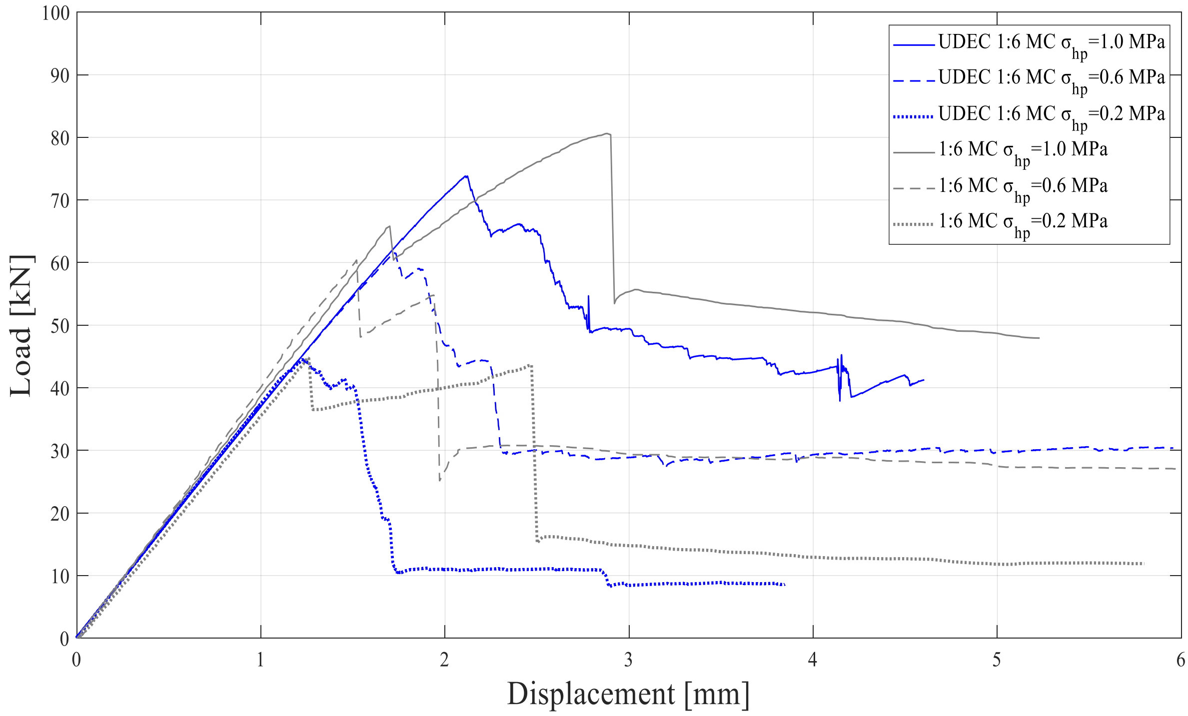

Figure 16. Experimental and numerical results of monotonic shear test on triplet with 1:6 MC

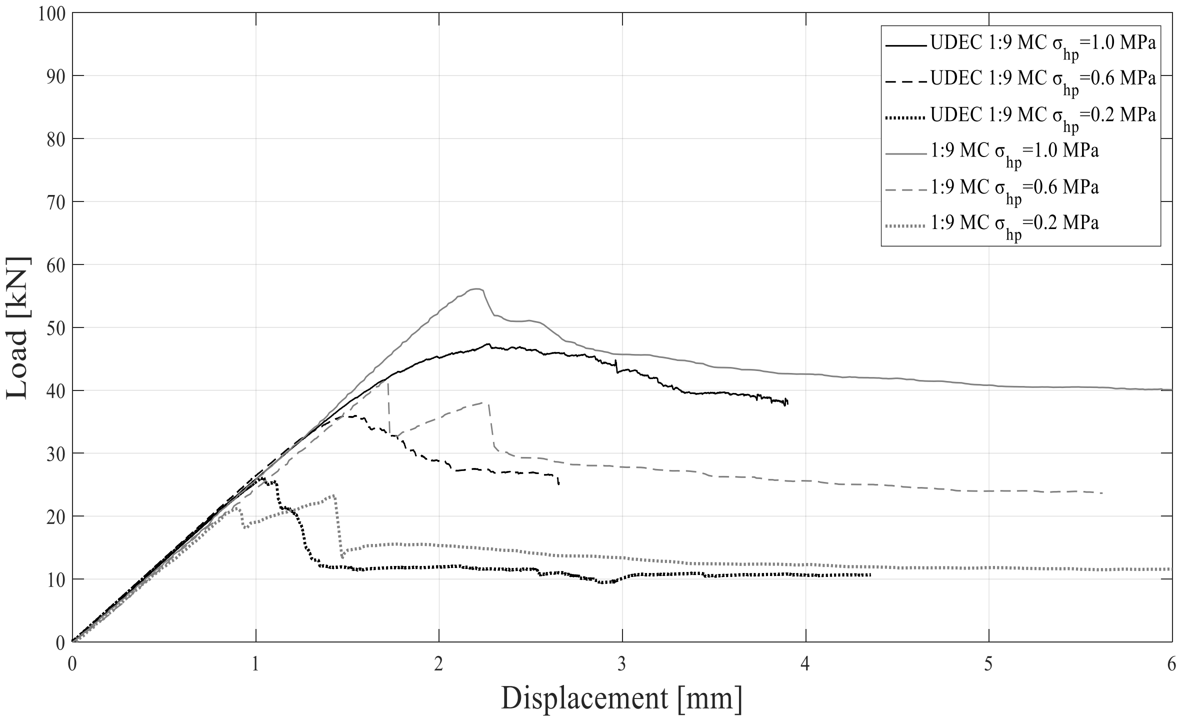

Figure 17. Experimental and numerical results of monotonic shear test on triplet with 1:9 MC

From Figures 15, 16 and 17, in both numerical simulations and experimental tests, both peak and residual strengths increase as the pre-compression stress increases. Similar findings were also reported by Abdou et al. (2006). Moreover, the masonry triplets constructed with 1:3 MC and 1:6 MC provide similar levels of stiffness and strength, while triplets constructed with 1:9 MC consistently exhibited the weakest mechanical performance. Figures 15, 16 and 17 show that most triplets exhibited experimentally a first sudden drop of shear strength before attaining the peak strength value. This behaviour is due to cracks forming in the mortar. With the application of further loading, the shear strength in the triplet increased until failure state reached. This occurred when cracks appeared in the mortar and brick to mortar interface of the triplet specimen. From the results analysis, it was shown that the peak strength of the specimen increases as the cement-to-sand ratio in the mortar increases. This is in agreement with results from the three-point bending tests and compressive strength tests performed on mortar specimens in the laboratory.

From Figures 15, 16, and 17 and Table 2, it appears that the residual strength is strongly affected by the pre-compression stress with a rather limited effect of the mortar composition. For instance, masonry triplets constructed with the mortar compositions 1:6 MC and 1:9 MC and with 0.6 MPa pre-compression showed a quite different peak loads (45% difference) but a rather similar residual shear strength (14% difference) to the one observed in the laboratory. Such behaviour was observed in both experimental and numerical studies carried out by the authors. Also, in the triplet tests, the two mortar joints are tested at the same time. These mortar joints do not fail concurrently but sequentially (as confirmed from both the experimental and numerical findings), which justifies the two peaks often found in the load against displacement curves in Figures 15 to 17.

Figures 18, 19 and 20 show the comparison of failure modes observed on masonry triplets made of mortar 1:3 MC in experimental and numerical tests, with precompression stresses of 0.2, 0.6 and 1 MPa, respectively. In the experiments, all masonry triplets exhibited failure at the mortar joints with individual bricks remaining intact at all times (Figures 18-c, 19-c and 20-c). In particular, the failure mechanism is characterised by slipping at the interface between the bricks and the mortar joints at the low precompression stress of 0.2 MPa (e.g. Figures 18a and 18b). As precompression stress increased, masonry triplets started exhibiting diagonal failure of the mortar joints, regardless of mortar composition (e.g. Figures 20a and 20b). This finding has been observed in both experimental tests and numerical simulations. This is in agreement also with EN 1052-3 (2002) that states that slipping at the brick-mortar interface and diagonal failure of the mortar joints are the most common failure mechanisms in masonry assemblages subjected to shear stress.

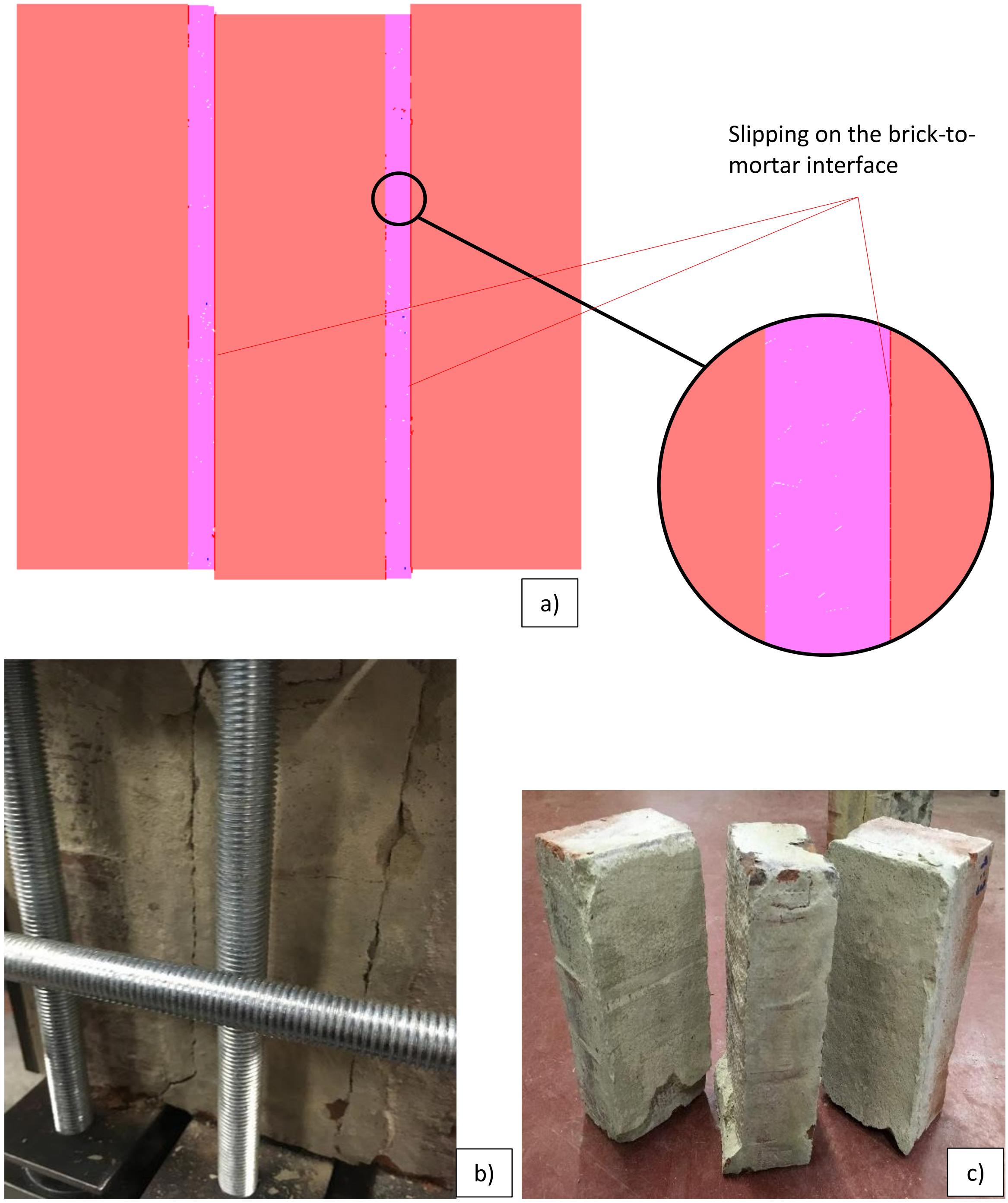

Figure 18. Failure mechanisms of masonry triplets 1:3 MC under monotonic shear tests at the precompression level of 0.2 MPa a) failure mode obtained from UDEC; b) crack forming during experimental tests; c) corresponding failed sample.

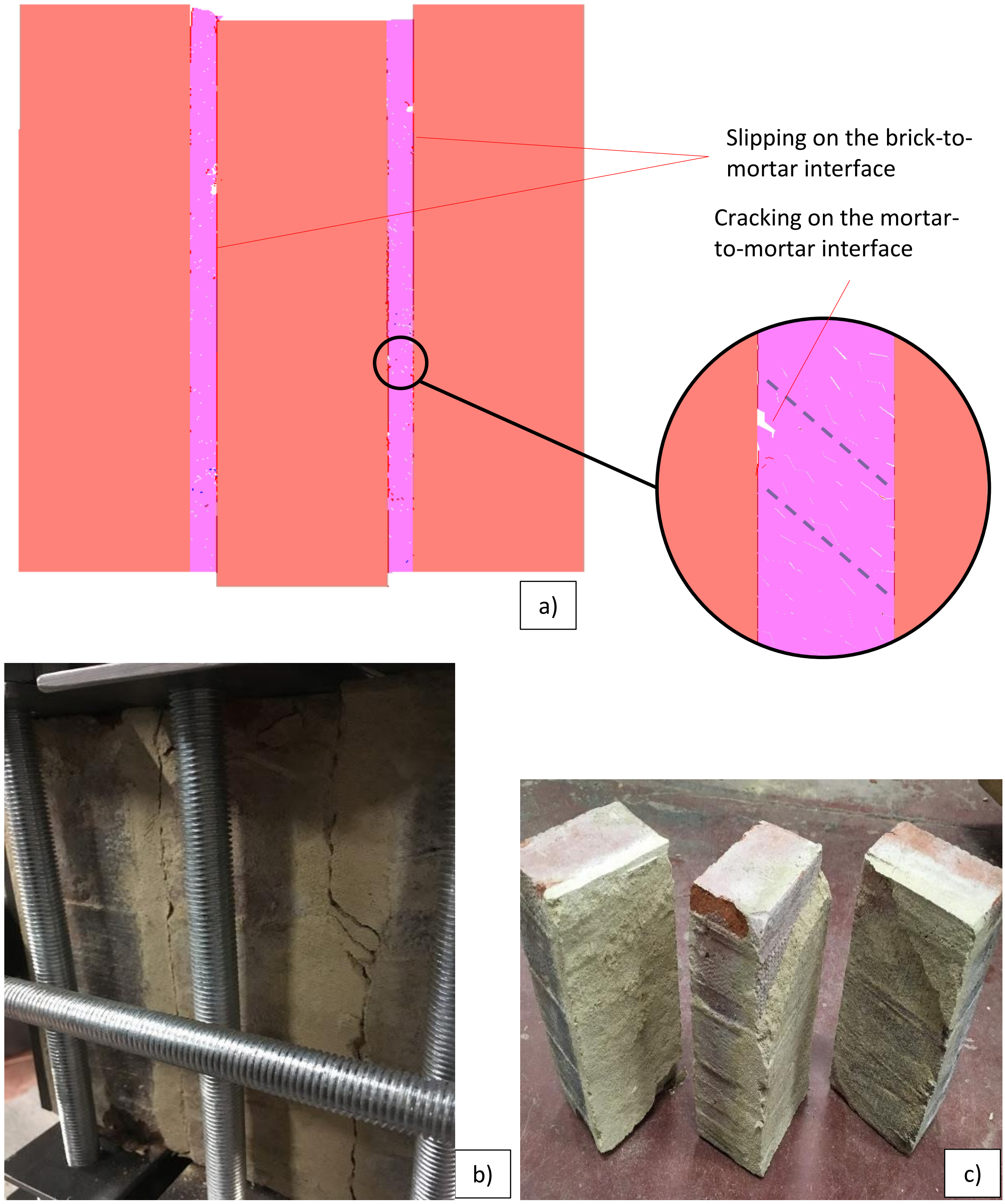

Figure 19. Failure mechanisms of masonry triplets 1:3 MC under monotonic shear tests at the precompression level of 0.6 MPa a) failure mode obtained from UDEC; b) crack forming during experimental tests; c) corresponding failed sample.

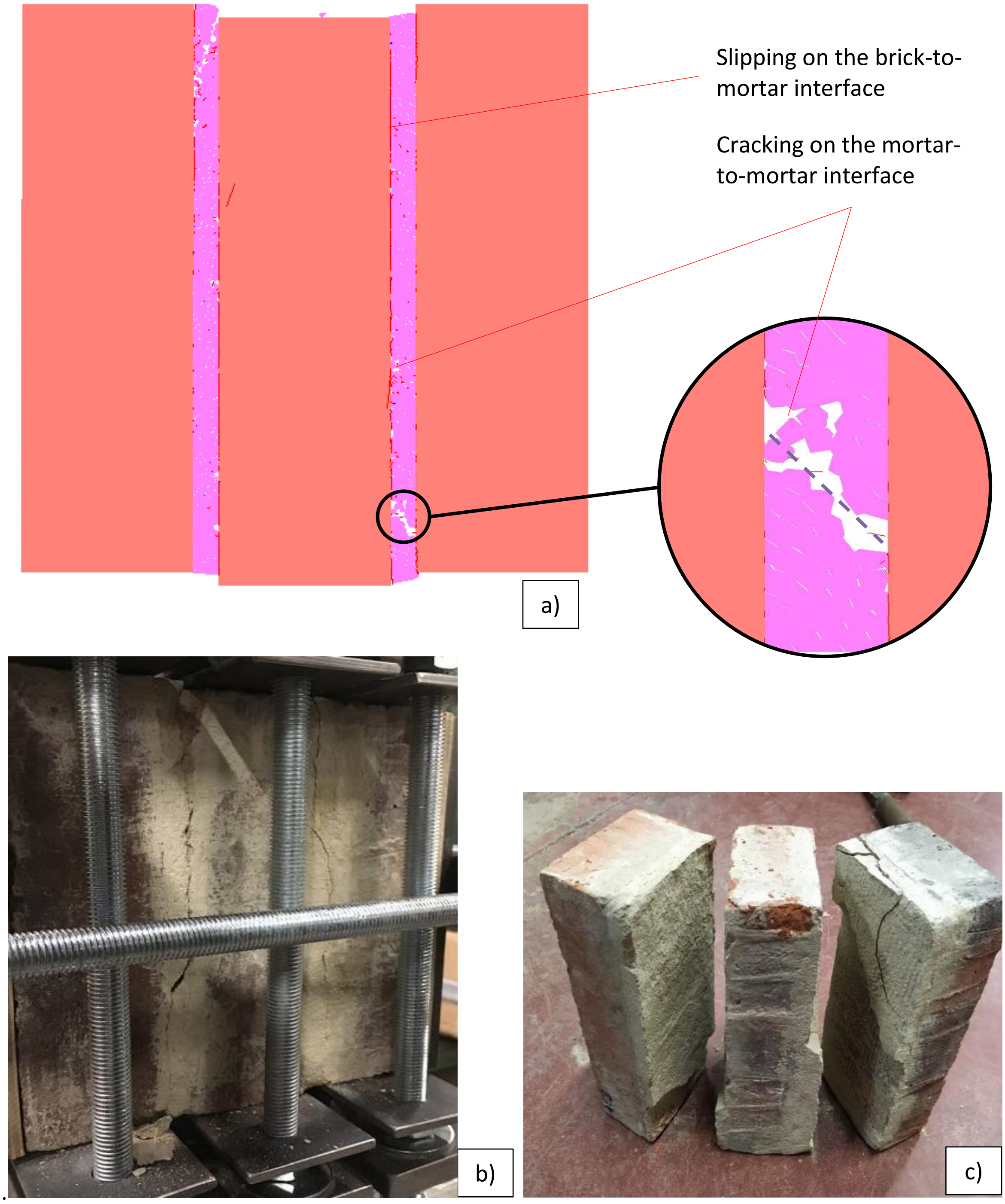

Figure 20. Failure mechanisms of masonry triplets 1:3 MC under monotonic shear tests at the precompression level of 1 MPa a) failure mode obtained from UDEC; b) crack forming during experimental tests; c) corresponding failed sample.

4.2 Cyclic shear tests

Figure 21 shows the experimental results from cyclic shear tests performed on masonry triplets bonded with three mortar compositions 1:3 MC, 1:6 MC and 1:9 MC together with results of the monotonic tests. From Figure 21 it can be noted that all masonry triplets exhibited very similar stiffness under both monotonic and cyclic shear tests. Also, it is shown that the shearing behaviour is relatively symmetric when shear loading is applied in both downward and upward directions. Also, from Figure 21 it can be observed that triplets tested under cyclic shear loading have a similar stiffness but reduced peak strength when compared with the ones tested under monotonic loading (see also Table 4 in Section 2.2.2). Notwithstanding this, the failure modes of the triplets tested under cyclic tests were very similar to those tested under monotonic loading. In particular, it was found that for a precompression stress equal to 0.2 MPa, the failure mode is characterised by slipping at the brick to mortar interface. As the precompression levels increased, a shear failure at the mortar was observed. Unlike monotonic tests, the force-displacement curves obtained during cyclic tests did not exhibit any preliminary drop of strength before failure. This can be due to micro-cracks occurred during cycling which resulted to a smoother force-displacement relationship compared with the monotonic tests. Additionally, the peak strength, measured under cyclic conditions, was attained at displacements consistently lower than those measured during monotonic tests. This can be associated to the accumulation of damages produced during cycling. Finally, it should be specified that, for experimental limitations, the post-peak behaviour could be investigated during cyclic tests only if the peak strength was achieved over the last cycle. During these tests (e.g. cyclic tests on mortar 1:6 at precompression stresses of 0.6 and 1 MPa), a good agreement between monotonic and cyclic behaviour is observed, thus suggesting that residual shear strength parameters are similar from both testing conditions.

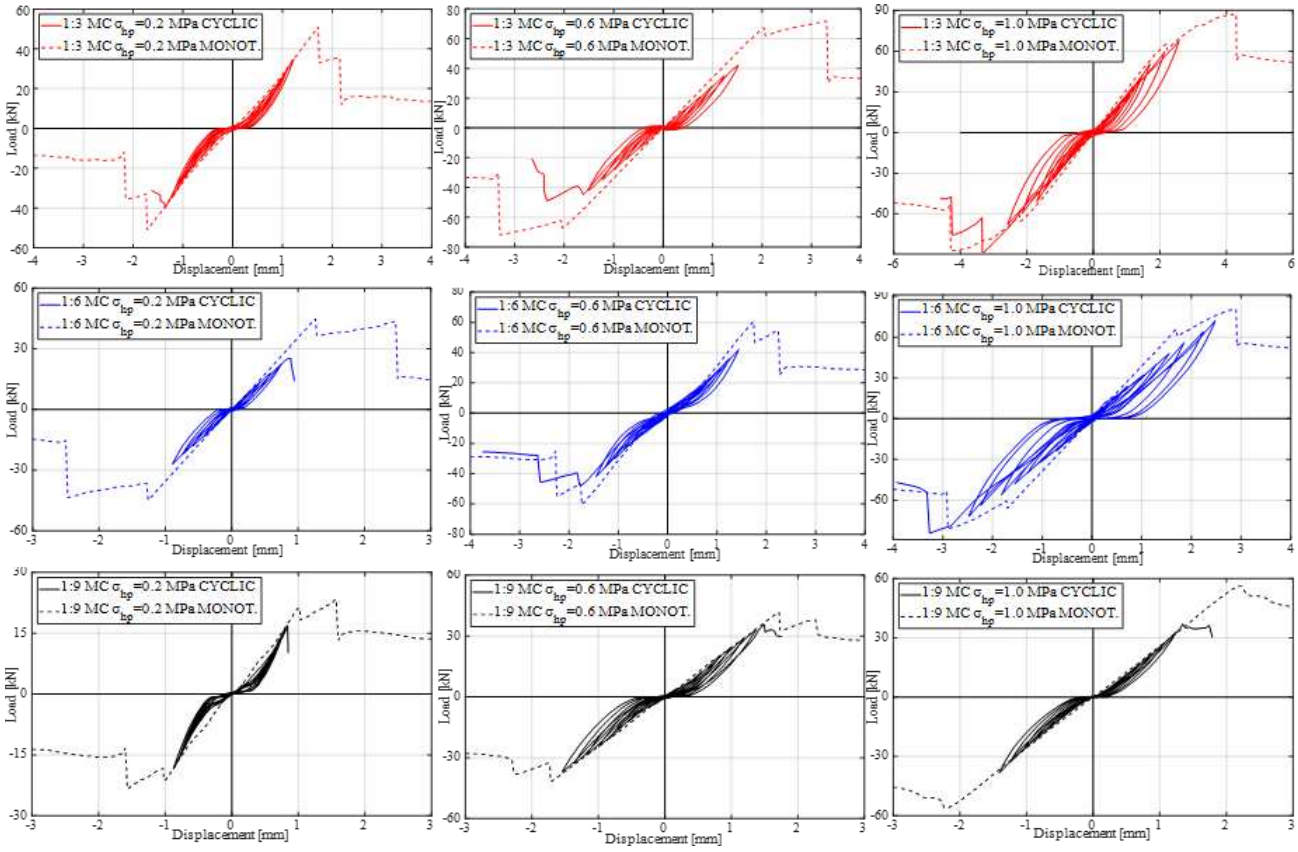

Figure 21. Cyclic and monotonic experimental shear test on triplets built with mortars 1:3 MC, 1:6 MC and 1:9 MC.

As regards as the numerical results, only two cases are shown for the sake of brevity, i.e. 1:6 MC triplets, with 0.2 and 0.6 MPa of pre-compression perpendicular to the mortar bed joint. Figures 22 and 23 show the results obtained from cyclic shearing tests on triplets with 1:6 MC and horizontal pre-stress equal to 0.2 and 0.6 MPa respectively. As can be noted, Figures 22 and 23 show the peak load variation that the masonry triplets exhibited passing from monotonic to cyclic loading conditions, while the stiffness does not show any significant change between the two load conditions (monotonic and cyclic).

Figure 24 shows the crack pattern of the cyclic shear test on the triplet with 1:6 MC and σ_{hp}=0.6 MPa, after the 7th, 8th, 9th and 10th cycles (Figures 24 a, b, c and d, respectively) as obtained from the numerical model. From Figure 24, with the application of external cyclic load, a progressive formation of cracking in the mortar is observed, with a gradual increase of the slipping and cracking at the mortar-to-mortar interfaces, which resulted to a lower shear strength value. Indeed, the cyclic action influences the peak shear strength, which shows a significant reduction (up to the 15%). Therefore, the peak shear strength reduction recorded in the simulation appears similar to what shown in the experimental tests, due to the formation of micro-fractures and local slipping between the Voronoi elements under cycling loading. At the end of the simulations (see Figure 26d), the failure modes of the triplets subjected to cyclic loading were similar to the ones observed during monotonic tests, i.e. mixed slipping and formation of diagonal cracks in the mortar.

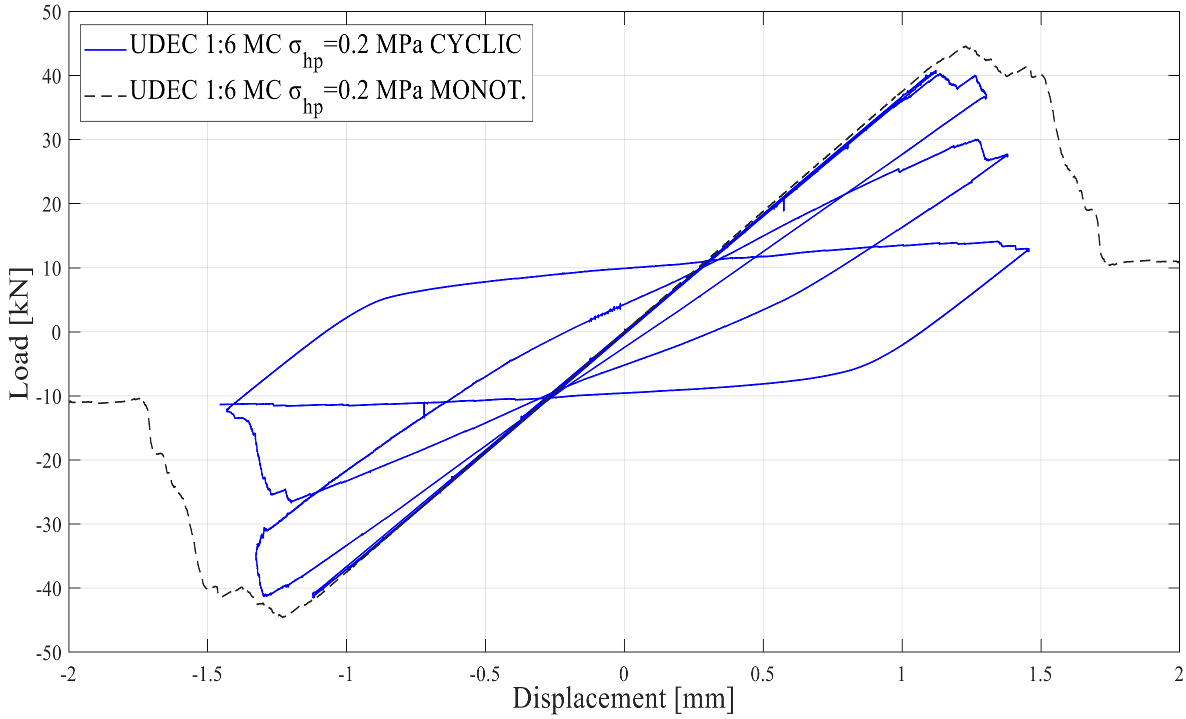

Figure 22. Numerical modelling results of cyclic shear test on masonry triplet 1:6 MC and σ_{hp}=0.2 MPa.

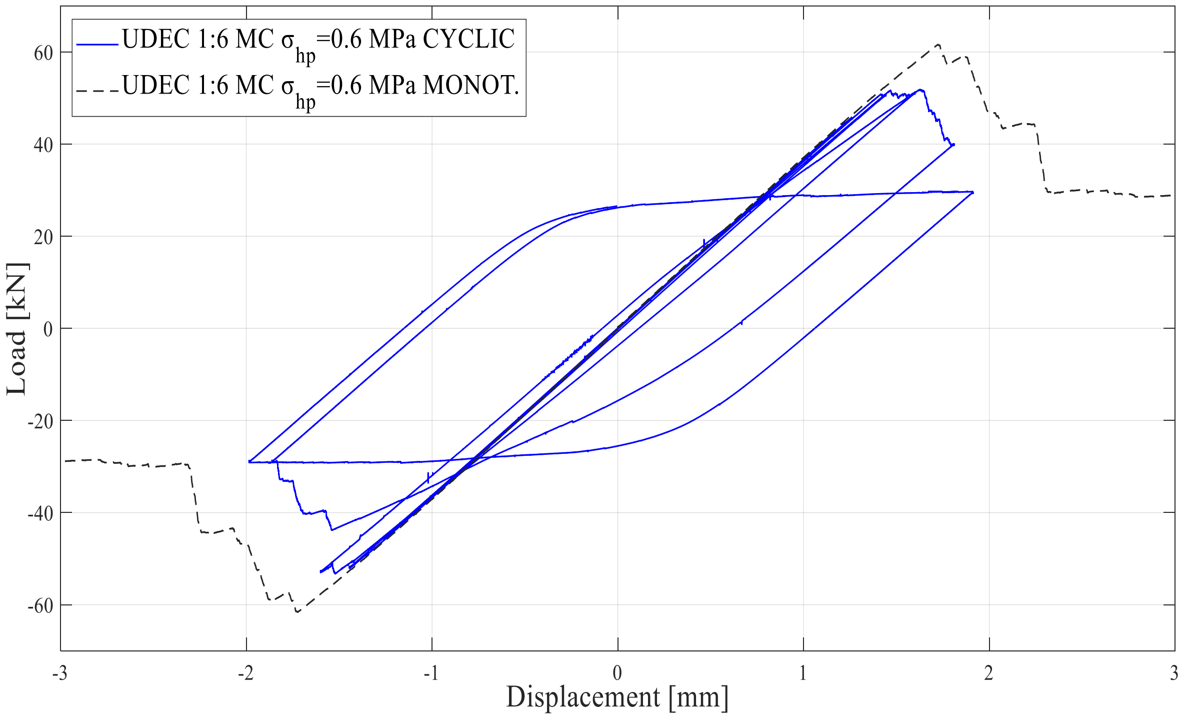

Figure 23. Numerical modelling results of cyclic shear test on masonry triplet 1:6 MC and σ_{hp}=0.6 MPa.

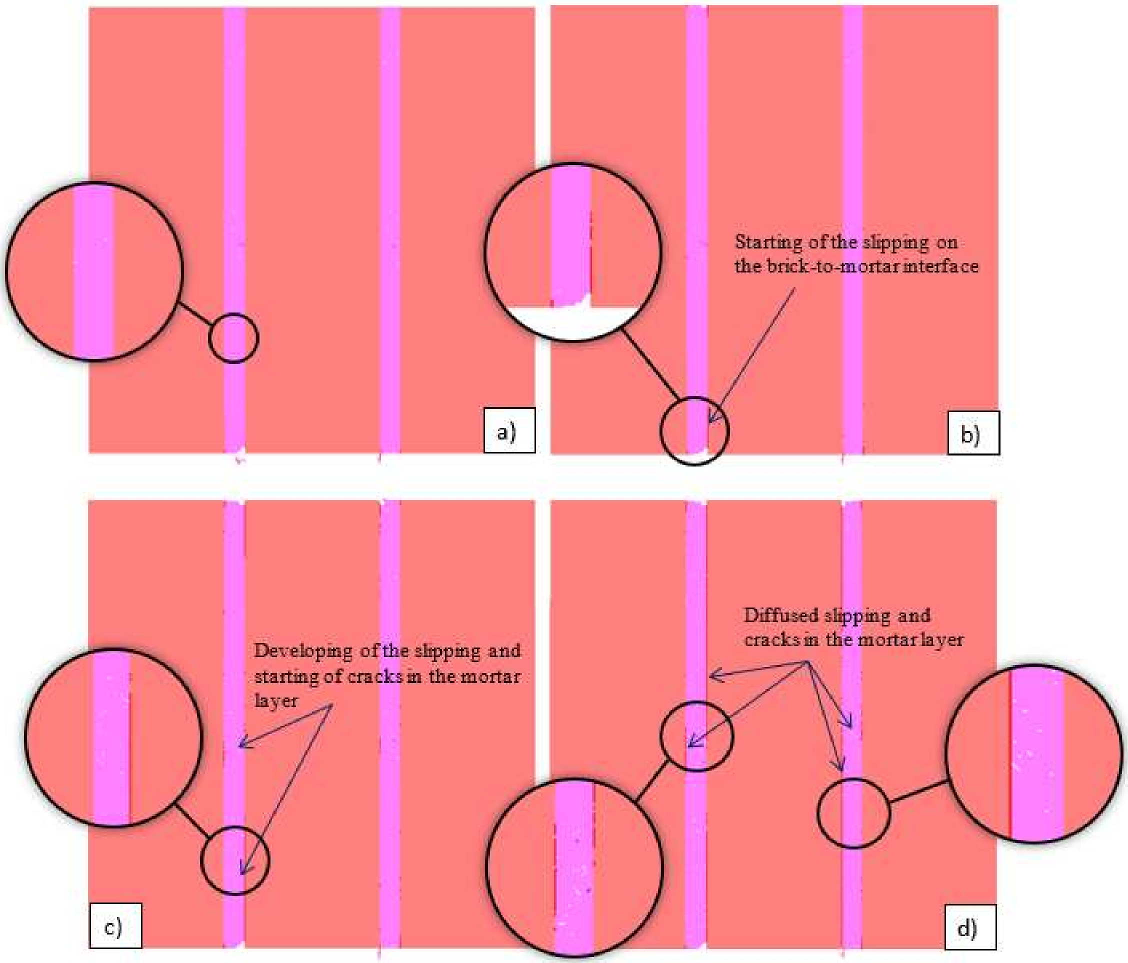

Figure 24 – Bed joint failire obtained after cyclic tests performed on triplet with 1:6 MC and σ_{hp}=0.6 MPa; a) specimen after 7th cycle; b) specimen after 8th cycle; c) specimen after 9th cycle; d) specimen after 10th cycle.

5. CONCLUSIONS

In this paper, both experimental and numerical strategies have been developed to study the shear response of masonry triplets under different levels of precompression and different mortar compositions. Moreover, two shear load conditions (i.e. monotonic and cyclic) were analysed. An original experimental apparatus was developed to impose both unidirectional and cyclic load condition to masonry triplet specimens, while an advanced numerical approach was developed able to capture the failure modes observed in the laboratory. Particularly, a DEM approach was developed to model mortar layers as an assemblage of densely packed discrete voronoi-shaped elements, bonded together by zero thickness interface laws. The load-displacement curves and failure modes obtained from the experimental tests were compared to the numerical results. From the discussion of the results, it is possible to conclude that:

- Results from monotonic shear tests indicated that the post-peak strength largely depended on the applied level of precompression stress whit a rather limited effect of the mortar composition.
- Masonry triplets exhibited a similar stiffness during both monotonic and cyclic shear tests.
- The peak shear strength observed during both monotonic and cyclic shear tests increased with increasing levels of precompression pressure and cement content.
- Significant shear strength reductions (typically around 18%) were observed for cyclic load conditions with respect to the monotonic ones for both experimental and numerical tests.
- The experimental and numerical failure modes of the masonry triplets showed a reasonably good agreement. Particularly, failure modes were influenced by the compression level, independently from the mortar joint properties, i.e. slipping occurred along with the brick-to-mortar interface for lower, while diagonal cracks developed in the mortar layers for higher

compression levels. Therefore, the compression level has been found to sensibly affect, beyond the shear response, the triplet failure mode.

- An overall good agreement between experimental and numerical results was obtained, showing a significant potential of the proposed non-standard DEM approach for simulating the discrete and highly non-linear behaviour of masonry structures.

It is envisaged that the current study provides an understanding of the cyclic shearing phenomena in masonry and thus could contribute towards the development of serviceability criteria for masonry structures subjected to loading.

ACKNOWLEDGEMENTS

The authors wish to acknowledge the support provided by the School of Engineering and the Geotechnics and Structures group of Newcastle University during the development of the experimental campaign shown in the paper.

REFERENCES

Abdou, L., Saada, R. A., Meftah, F., & Mebarki, A. (2006). Experimental investigations of the joint-mortar behaviour. Mechanics research communications, 33(3), 370-384.

Alecci, V., Fagone, M., Rotunno, T., & De Stefano, M. (2013). Shear strength of brick masonry walls assembled with different types of mortar. Construction and Building Materials, 40, 1038-1045.

Andreotti, G., Graziotti, F., & Magenes, G. (2018). Detailed micro-modelling of the direct shear tests of brick masonry specimens: the role of dilatancy. Engineering Structures, 168, 929-949.

ASTM. (2003). "Standard test method for compressive strength of masonry prisms." C1314-03b, West Conshohocken, PA.

Bertolesi E., Milani G., Casolo S. (2018). Homogenization towards a mechanistic Rigid Body and Spring Model (HRBSM) for the non-linear dynamic analysis of 3D masonry structures. Meccanica, 53, pp. 1819-1855.

Bertolesi E., Milani G., Lourenço P.B. (2016). Implementation and validation of a total displacement non-linear homogenization approach for in-plane loaded masonry. Computers & Structures, 176, pp. 13-33.

Bertolesi E., Silva L.C., Milani G. (2019). Validation of a two-step simplified compatible homogenisation approach extended to out-plane loaded masonries. International Journal of Masonry Research and Innovation 4(3) pp. 265-296.

Bui, T.T., Limam, A, Sarhosis, V., Hjiajd, M. (2017). Discrete element modelling of the in-plane and out-of-plane behaviour of dry-joint masonry wall constructions, Engineering Structures, 136, 277–294

Capozucca, R. (2011). Shear behaviour of historic masonry made of clay bricks. Open Construction and Building Technology Journal, 5, 89-96.

Capozucca, R. (2017). Experimental response of historic brick masonry under biaxial loading. Construction and Building Materials, 154, 539-556.

Casolo, S., & Milani, G. (2013). Simplified out-of-plane modelling of three-leaf masonry walls accounting for the material texture. Construction and Building Materials, 40, 330-351.

D'Altri, A. M., de Miranda, S., Castellazzi, G., & Sarhosis, V. (2018). A 3D detailed micro-model for the in-plane and out-of-plane numerical analysis of masonry panels. Computers & Structures, 206, 18-30.7

D’Altri, A. M., Sarhosis, V., Milani, G., Rots, J., Cattari, S., Lagomarsino, S., Sacco, E., Tralli, A., Castellazzi, G., & de Miranda, S. (2019). Modeling Strategies for the Computational Analysis of Unreinforced Masonry Structures: Review and Classification. Archives of Computational Methods in Engineering, 1-33.

Dehghan, S. M., Najafgholipour, M. A., Baneshi, V., & Rowshanzamir, M. (2018). Mechanical and bond properties of solid clay brick masonry with different sand grading. Construction and Building Materials, 174, 1-10.

Drysdale, R., Hamid, A., and Baker, L. (1999). Masonry structures: Behaviour and design, The Masonry Society, Boulder, CO.

EN 1015-11 (1999). Methods of test for mortar for masonry. Determination of flexural and compressive strength of hardened mortar. European Committee for Standardization: Brussels, Belgium.

EN 1052-3 (2002). Methods of test for masonry-Part 3: Determination of initial shear strength. European Committee for Standardization: Brussels, Belgium.

Eurocode 6 (2005). Design of masonry structures. British Standard Institution, London.

Ferretti, F., Ferracuti, B., Mazzotti, C., & Savoia, M. (2019). Destructive and minor destructive tests on masonry buildings: Experimental results and comparison between shear failure criteria. Construction and Building Materials, 199, 12-29.

Franzoni, E., Gentilini, C., Graziani, G., & Bandini, S. (2014). Towards the assessment of the shear behaviour of masonry in on-site conditions: a study on dry and salt/water conditioned brick masonry triplets. Construction and Building Materials, 65, 405-416.

Ghazvinian, E., Diederichs, M. S., & Quey, R. (2014). 3D random voronoi grain-based models for simulation of brittle rock damage and fabric-guided micro-fracturing. Journal of Rock Mechanics and Geotechnical Engineering, 6(6), 506-521.

Itasca (2004). UDEC – Universal Distinct Element Code, Users Manual, Minneapolis, USA.

Konthesingha, K. M. C., Jayasinghe, C., & Nanayakkara, S. M. A. (2007). Bond and compressive strength of masonry for locally available bricks. Engineer: Journal of the Institution of Engineers, Sri Lanka, 40(4).

Leknitskii, S. G. (1963). Theory of elasticity of an anisotropic elastic body. Holden-day.

Lin, K., Liu, H., Wei, C., & Huang, Q. (2017). Effects of shear rate on cyclic behavior of dry stack masonry joint. Construction and Building Materials, 157, 809-817.

Livitsanos, G., Shetty, N., Verstrynge, E., Wevers, M., Van Hemelrijck, D., & Aggelis, D. G. (2019). Shear failure characterization in masonry components made with different mortars based on combined NDT methods. Construction and Building Materials, 220, 690-700.

Lourenço, P. B. (2002). Computations on historic masonry structures. Progress in Structural Engineering and Materials, 4(3), 301-319.

Lourenço, P. B., Barros, J. O., & Oliveira, J. T. (2004). Shear testing of stack bonded masonry. Construction and Building Materials, 18(2), 125-132.

Milani, G. (2009). Homogenized limit analysis of FRP-reinforced masonry walls out-of-plane loaded. Computational Mechanics, 43(5), 617-639.

Milani, G. (2011). Simple lower bound limit analysis homogenization model for in-and out-of-plane loaded masonry walls. Construction and Building Materials, 25(12), 4426-4443.

Milosevic, J., Gago, A. S., Lopes, M., & Bento, R. (2013). Experimental assessment of shear strength parameters on rubble stone masonry specimens. Construction and Building Materials, 47, 1372-1380.

Mojsilović, N. (2012). Masonry elements with damp-proof course membrane: Assessment of shear strength parameters. Construction and Building Materials, 35, 1002-1012.

Mojsilović, N., Petrović, M., & Anglada, X. R. (2015). Masonry elements with multi-layer bed joints: Behaviour under monotonic and static-cyclic shear. Construction and Building Materials, 100, 149-162.

Mojsilović, N., Petrović, M., & Stojadinović, B. (2019). Multi-layer masonry bed joint subjected to shear: Analytical modelling. Construction and Building Materials, 205, 602-610.

Pelà, L., Kasioumi, K., & Roca, P. (2017). Experimental evaluation of the shear strength of aerial lime mortar brickwork by standard tests on triplets and non-standard tests on core samples. Engineering Structures, 136, 441-453.

Pluijm, van der, R. (1993). Shear behaviour of bed joints. In A. A. Hamid, & H. G. Harris (Eds.), 6th North American Masonry Conference, 6-9 June 1993, Philadelphia, Pennsylvania, USA (pp. 125-136). Lancaster: Technomic Publ. Co..

Rahman, A., & Ueda, T. (2013). Experimental investigation and numerical modeling of peak shear stress of brick masonry mortar joint under compression. Journal of Materials in Civil Engineering, 26(9), 04014061.

Sarangapani, G., Venkatarama Reddy, B. V., & Jagadish, K. S. (2005). Brick-mortar bond and masonry compressive strength. Journal of materials in civil engineering, 17(2), 229-237.

Sarhosis, V., & Lemos, J. V. (2018). A detailed micro-modelling approach for the structural analysis of masonry assemblages. Computers & Structures, 206, 66-81.

Sarhosis, V., & Sheng, Y. (2014). Identification of material parameters for low bond strength masonry. Engineering Structures, 60, 100-110.

Sarhosis, V., Bagi, K., Lemos, J.V. & Milani, G. (2016). Computational modelling of masonry structures using the discrete element method. IGI Global.

Silva L.C., Lourenço P.B., Milani G. (2017). Rigid block and spring homogenized model (HRBSM) for masonry subjected to impact and blast loading. International Journal of Impact Engineering, 109, pp. 14-28.

Singh, S. B., Munjal, P., & Thammishetti, N. (2015). Role of water/cement ratio on strength development of cement mortar. Journal of Building Engineering, 4, 94-100.

Van Zijl, G. P. (2004). Modeling masonry shear-compression: Role of dilatancy highlighted. Journal of engineering mechanics, 130(11), 1289-1296.

Zhuge, Y. (1998). The behaviour of masonry walls containing a damp-proof course under cyclic loads (Doctoral dissertation, Structural Engineering Society of New Zealand).